



ELSEVIER

Thermochimica Acta 321 (1998) 99–109

thermochimica
acta

Thermal and morphological analysis of isotactic poly(1-butene)/hydrogenated oligocyclopentadiene blends

S. Cimmino, M.L. Di Lorenzo*, C. Silvestre

Istituto di Ricerca e Tecnologia delle Materie Plastiche, CNR, Via Toiano 6, Arco Felice, 80072 Naples, Italy

Received 24 March 1997; accepted 1 December 1997

Abstract

This contribution discusses the influence of hydrogenated oligocyclopentadiene (HOCP) on the morphology, the phase structure and the thermal properties of its blends with isotactic poly(1-butene) (PB-1) as a function of composition and crystallization conditions.

PB-1 and HOCP are partially miscible in the melt state. The blends, in the solid state, form generally a three-phase system: a crystalline phase formed by the polyolefin and two amorphous phases, of which one is rich in PB-1 and the other one in HOCP. The optical micrographs of the solidified blends show a morphology constituted by microspherulites and domains of HOCP-rich phase homogeneously distributed in intraspherulitic regions. Moreover, when the PB-1 and the blends are isothermally crystallized, hedrite-like crystallites are observed.

The crystallization process and the melting behavior are strongly influenced by the presence of the oligomer, since the addition of HOCP decreases the overall crystallization rate and the melting point of the blends. © 1998 Elsevier Science B.V.

Keywords: Crystallization; DMTA; DSC; Hydrogenated oligocyclopentadiene; Miscibility; Morphology; Poly(1-butene); Thermal properties

1. Introduction

Isotactic poly(1-butene) (PB-1) is a semicrystalline polyolefin with some interesting properties. Properly molded and processed articles made by poly(1-butene) show excellent resistance to creep and environmental stress cracking [1]. Extruded PB-1 is in fact mainly used in the manufacture of pipes and tubes because of its impact and corrosion resistance. But other products, such as heavy duty bags, pressure sensitive tapes, agricultural films, gaskets and diaphragms can also be obtained. In certain cases, such as applica-

tions at low temperature, where high impact resistance is needed, PB-1 is preferred to isotactic polypropylene (iPP) and poly(4-methylpentene-1) (P4MP1) for the production of house furnishing, electrical apparatus, automotive parts and other articles [2].

The oligocyclopentadiene is obtained by oligomerization of cyclopentadiene, which is present in coal tar and petroleum and occurs in the lower boiling fractions. Thermal oligomerization is conducted at temperatures above 200°C, and the molecular weight of the product is quite low (500 to 800). The commercial HOCP is a mixture of the *cis* and *trans* isomers that have been hydrogenated after oligomerization. It is a solid, white in color and glass brittle at room temperature.

*Corresponding author. Tel.: +39-81-8534174; fax: +39-81-8663378; e-mail: diloren@mail.irtemp.na.cnr.it

This work is part of a larger project that involves the study of the miscibility, the phase structure, the morphology and the thermal and mechanical properties of different polyolefins ($\text{CH}_2=\text{CHR}$) blended with hydrogenated oligocyclopentadiene, when the dimension of the group R is varied.

HDPE (the R group is a hydrogen atom) and HOCP have been found to be partially miscible in the melt phase [3,4]; at room temperature there are three phases: a crystalline phase constituted by plain HDPE and two amorphous phases, one rich in HDPE and the other one rich in HOCP. The iPP/HOCP system ($\text{R}=\text{CH}_3$) presents a higher degree of miscibility, since for $T>240^\circ\text{C}$ and $T<90^\circ\text{C}$ the two components are miscible, whereas a miscibility gap is present between these two temperatures [5–8]. Therefore, depending on composition and thermal conditions, at room temperature two or three phases can be present. On the other hand, P4MP1 and HOCP (the R group is a $\text{CH}_2\text{CH}(\text{CH}_3)_2$) are completely immiscible in the melt phase [9].

Both the polyolefins and the oligomer have a hydrocarbon structure, specific interactions between components are not possible, therefore the differences in the miscibility of the various polymer pairs can be ascribed only to differences in the volume units of the components [10].

The R group of PB-1 is a CH_2CH_3 , with steric hindrance between that of iPP and that of P4MP1, so the miscibility of the PB-1/HOCP system is expected to be between that of the polymer pairs iPP/HOCP and P4MP1/HOCP. It is noteworthy that the studies on the binary blend iPP/HOCP lead to very interesting results: the addition of small amounts of HOCP to iPP gives a material with improved properties compared to pure iPP [11,12].

The objectives of this paper are the study of the miscibility, the phase structure and thermal properties of PB-1/HOCP blends, as well as the influence of HOCP on the crystallization process of PB-1.

2. Experimental

2.1. Materials

Isotactic poly(1-butene) was produced by Scientific Polymer Products. Its physical values were $M_w=1.85\times 10^5$ (g mol^{-1}), density 0.915 (g cm^{-3}), Melt

index 20, $T_g=-23\pm 3^\circ\text{C}$ (measured by DSC) and $T_m=125^\circ\text{C}$ (form I) (measured by DSC).

The hydrogenated mixture of isomers of oligocyclopentadiene (HOCP), Escorez 5120 was produced by Esso Chemical. Its physical values were $M_w=630$ (g mol^{-1}), $T_g=85\pm 3^\circ\text{C}$ (measured by DSC) and density 1.07 (g cm^{-3}).

2.2. Blend preparation

The PB-1 and HOCP components were mixed in a Brabender-like apparatus (Rheocord EC of HAAKE) at 160°C and 32 rpm for 10 min. PB-1/HOCP blends with weight ratios (w/w) of 100/0, 90/10, 80/20, 60/40 and 40/60 were prepared.

2.3. Preparation of compression-molded sheets

The blends were compression-molded in a heated press at 160°C for 5 min without any applied pressure, to allow complete melting. After this period, a pressure of 100 bar was applied for 5 min, then the samples were quenched with water and the pressure was released. From the mold, parallelepiped shaped sheets ($1\text{ mm}\times 60\text{ mm}\times 120\text{ mm}$) were obtained.

2.4. Optical microscopy

The morphology of the blends was studied by using a Zeiss polarizing optical microscope, fitted with a Linkam TH600 hot stage. Thin films were obtained by squeezing a thin slice of compression-molded sheet between two microscope cover glasses. The films so obtained were then heated and cooled under nitrogen purge at $20^\circ\text{C}/\text{min}$.

2.5. Calorimetric measurements

The thermal properties of the blends were analyzed with a Mettler DSC-30 differential scanning calorimeter. Nearly 10–15 mg of each blended sample was heated from -80°C to 200°C at a scanning rate of $20^\circ\text{C}/\text{min}$ (first heating run), cooled to -80°C at $50^\circ\text{C}/\text{min}$ and re-heated to 200°C at $20^\circ\text{C}/\text{min}$ (second heating run). The T_g value was taken as the temperature corresponding to the maximum of the peak obtained by the first-order derivative trace of the second heating run.

The isothermal crystallizations were performed by using the following procedure. The samples were heated from 30° to 160°C at a scanning rate of 20°C/min, melted at 160°C for 10 min, then rapidly cooled at 50°C/min to the desired T_c and allowed to crystallize. The heat evolved during the isothermal crystallization was recorded as a function of time. The fraction X_t of the material crystallized after a period of time t was calculated by the relation:

$$X_t = \frac{\int_0^t (dH/dt) dt}{\int_0^\infty (dH/dt) dt}$$

where the first integral is the heat generated at time t and the second one is the total heat when the crystallization is complete.

After crystallization, the samples were heated to the melting point at a scanning rate of 20°C/min. The observed melting temperatures and the apparent enthalpies of melting were obtained from the maximum and from the area of the endothermic peaks, respectively.

2.6. Dynamic-mechanical tests

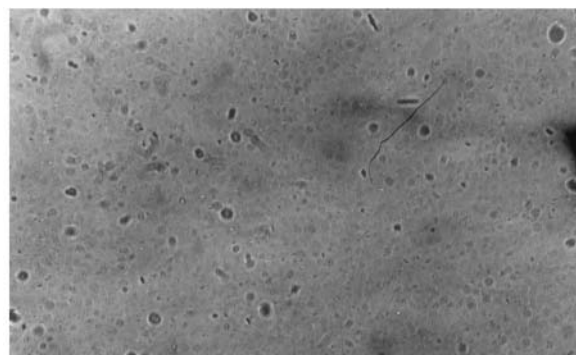
Parallelepiped shaped specimens (1 mm×6 mm×30 mm) were cut from the compression-molded sheets. Dynamic-mechanical tests were collected at 1 Hz and at a heating rate of 4°C/min from –80° to 100°C under nitrogen purge with a Polymer Laboratories DMTA MKIII tester configured for automatic data acquisition. The experiments were performed in bending mode.

3. Results and discussion

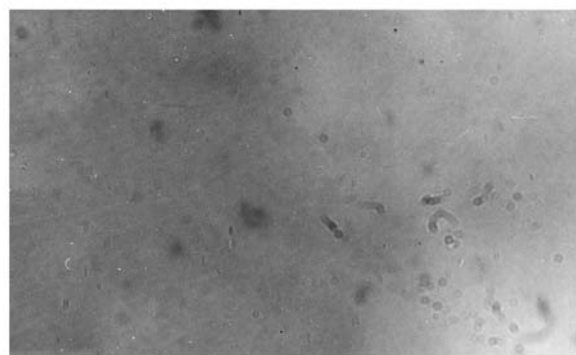
3.1. Morphology

Optical analyses of the melt of pure PB-1 and blends were carried out from the melting point up to 350°C, where all the samples are still thermally stable under nitrogen atmosphere for much longer times than those used here for the optical observations.

The phase structure of the PB-1/HOCP system depends on composition and temperature. Optical micrographs of the 90/10 blend at different temperatures are shown in Fig. 1. Up to ca. 250°C, the melt of



a)



b)

Fig. 1. Optical micrographs of PB-1/HOCP 90/10 blend film: (a) sample at 200°C; (b) sample at 300°C.

the 90/10 sample showed the presence of small droplets homogeneously distributed in the matrix (see Fig. 1(a)). The droplets decreased in size when the temperature was raised above 250°C. At ca. 270°C the melt became homogeneous and transparent and the homogeneity was preserved up to 350°C (see Fig. 1(b)). The droplets appeared again at ca. 270°C when the sample was cooled down from 350°C.

Optical micrographs of the 80/20, 60/40 and 40/60 (w/w) blends in the melt at 250°C are reported in Fig. 2. The melts of these blends are characterized by the presence of numerous droplets, whose dimensions increase with HOCP content. For these blends, the droplets did not disappear in the range of temperature used.

The morphology of PB-1 and of the blends cooled from the melt phase ($T=250^\circ\text{C}$) to room temperature

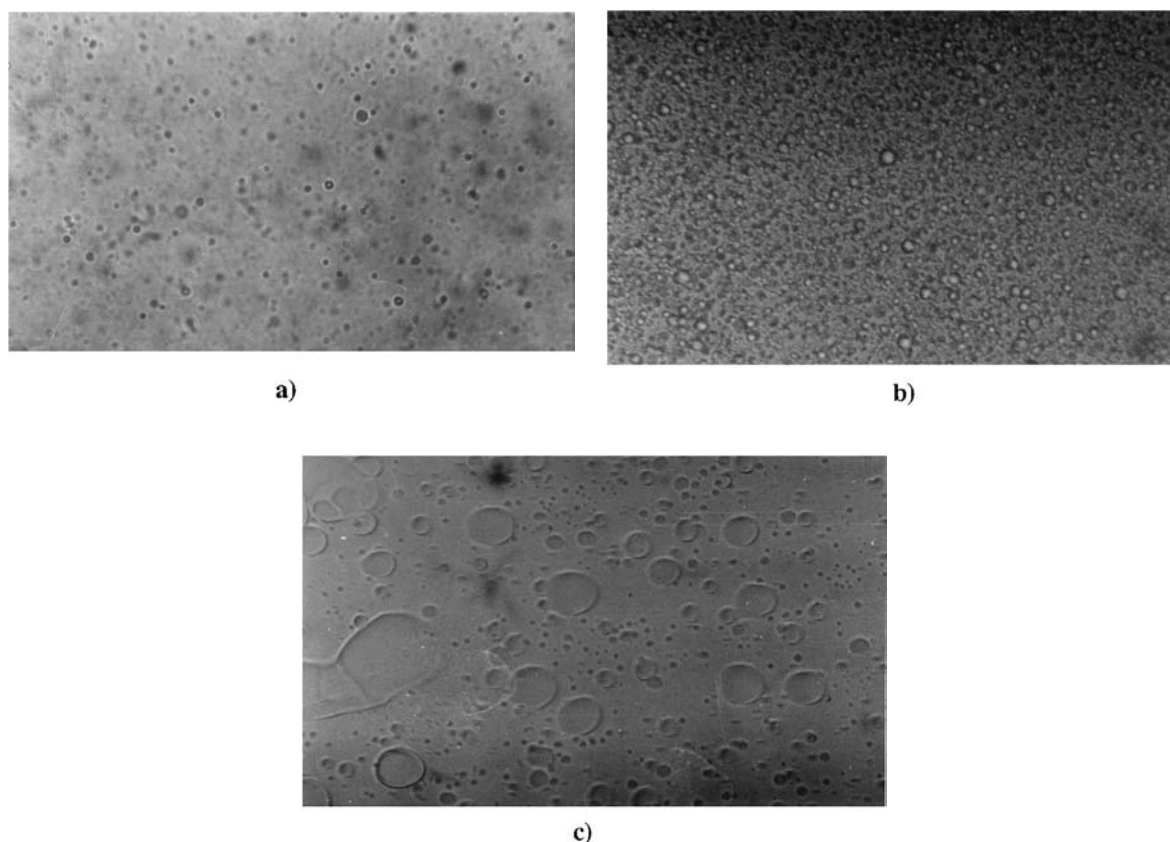


Fig. 2. Optical micrographs of PB-1/HOCP blend films at 250°C: (a) 80/20; (b) 60/40; (c) 40/60.

at 20°C/min is reported in Fig. 3. PB-1 crystallized prevalently to a spherulitic morphology. The spherulites were of different sizes (Fig. 3(a)). This phenomenon is known to occur when the nucleation process is time and temperature dependent. In fact, during cooling, the presence of few nuclei at high temperatures induce the formation of early spherulites that can grow. These are the large spherulites present in Fig. 3(a). Then, at lower temperatures, many nuclei induce the growth of many spherulites, that cannot grow to as large an extension as the early ones, because they are numerous and so impinge against each other.

When the 90/10 sample was cooled to room temperature, large and small spherulites were also observed, but they are coarse and much smaller than pure PB-1 (see Fig. 3(b)). Moreover, observations with crossed and parallel polars indicate that the

crystals grew within a liquid–liquid phase separated melt, as that shown in Fig. 1(a), and the droplets of the HOCP-rich phase were mainly included in intra-spherulitic regions during the crystallization.

The 60/40 blend (see Fig. 3(c)) presents a morphology constituted by microspherulites and droplets homogeneously distributed. A similar morphology was observed for the 40/60 blend.

When the blends were isothermally crystallized, besides spherulites, crystallites with different morphologies were also observed. In Fig. 4, two examples of growing crystals of PB-1 at 80°C are shown. The Fig. 4(a) shows a typical example of a spherulite with the characteristic Maltese cross and a circular section. In the same sample, square crystals are also observable (see Fig. 4(b)). These crystals are clearly different from the previous ones; they do not have the typical appearance of a spherulite, but they

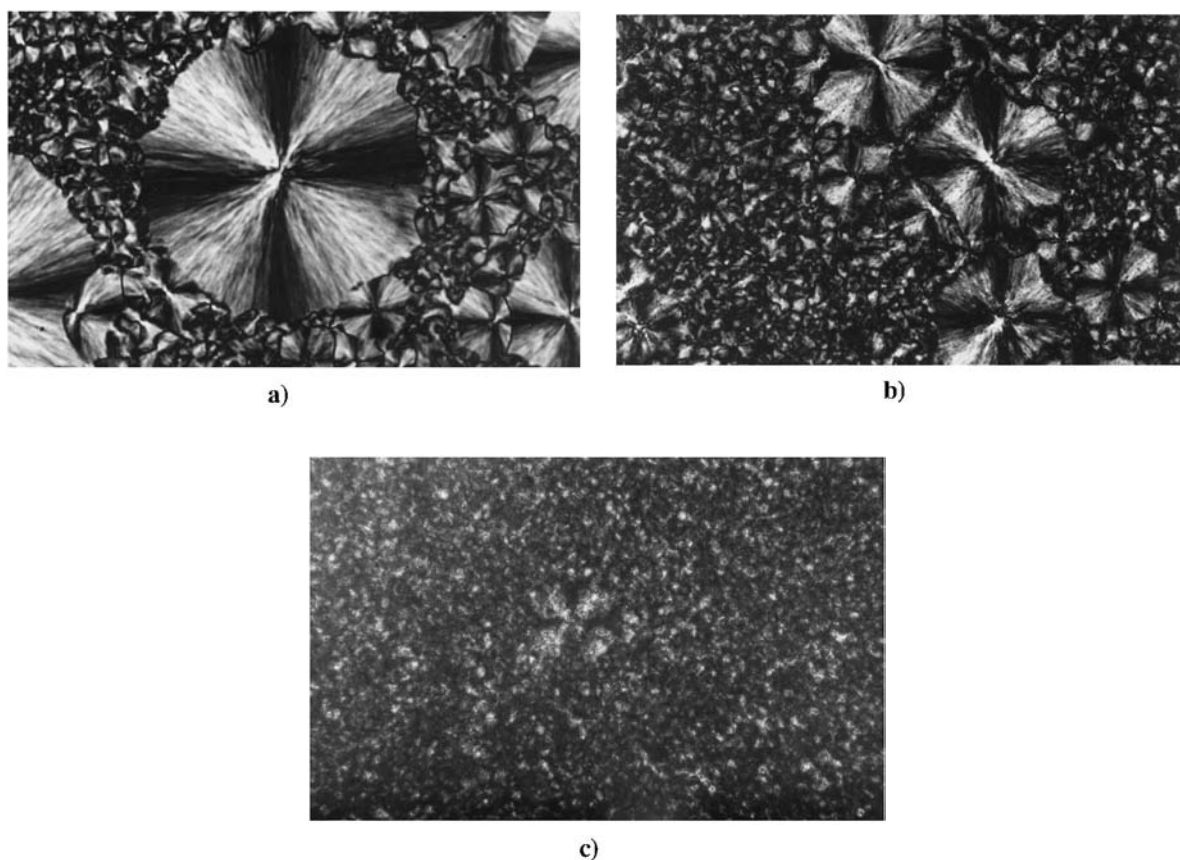


Fig. 3. Optical micrographs of PB-1/HOCP blend films at 25°C: (a) 100/0; (b) 90/10; (c) 60/40.

have hedritic character. Hedrites have been found for several polymers, including polymethylene oxide [13,14], isotactic polystyrene and poly(4-methylpentene-1) [15]. They are made of several lamellar layers and have a two-dimensional growth.

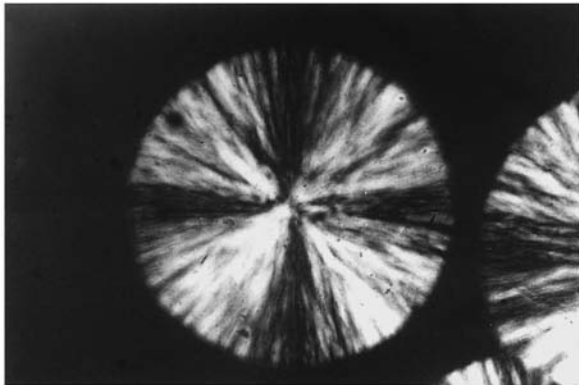
In all blends the presence of both kinds of crystallites are also observed. The photomicrographs of hedrites of the 80/20 and 60/40 blends are reported in Fig. 5 and, in the same blends, spherulites are also observable (see Fig. 3). It can be concluded that HOCP did not affect the morphology of PB-1 crystallites.

3.2. Glass-transition temperature

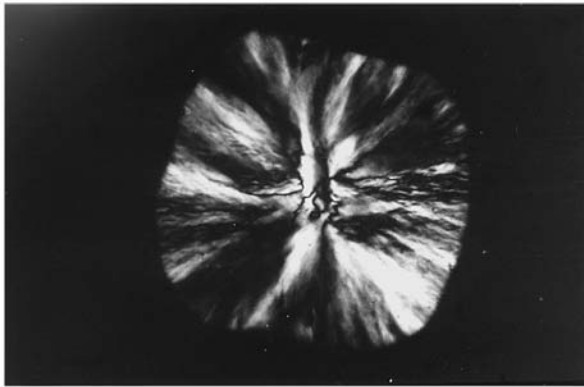
In order to analyze the composition of the amorphous phases of the blends, i.e. if the phases are

composed of the pure components, or if they are conjugated, the determination of glass-transition temperature (T_g) of each blend was performed by means of dynamic-mechanical thermal analysis (DMTA) and differential scanning calorimetry (DSC).

The $\tan \delta$ curves of PB-1/HOCP blends are reported in Fig. 6. DMTA experiments of pure HOCP could not be performed since it is not possible to obtain HOCP samples by compression molding because of its low molecular mass. The PB-1 curve presents a single peak with a maximum at -5°C which represents the T_g of PB-1. The 90/10 blend still presents one peak, but the size of this peak is smaller than that of PB-1 and it is shifted to a slightly higher temperature (the maximum is at $+5^\circ\text{C}$). In the $\tan \delta$ curve of the 80/20 blend, two peaks are detected: the first one is situated at slightly higher temperatures with respect to those of

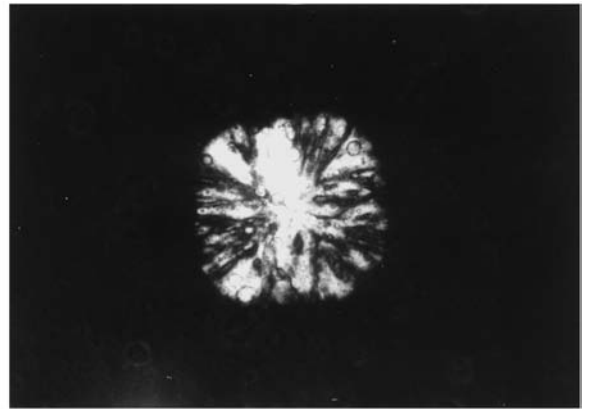


a)

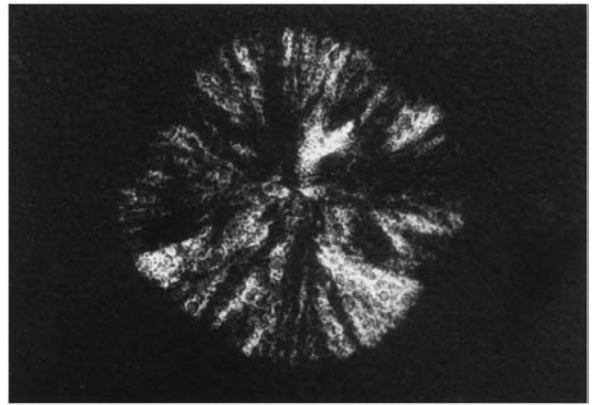


b)

Fig. 4. Optical micrographs of PB-1 crystallites isothermally crystallized at 80°C.



a)



b)

Fig. 5. Optical micrographs of PB-1/HOCP blend hedrites: (a) 80/20; (b) 60/40.

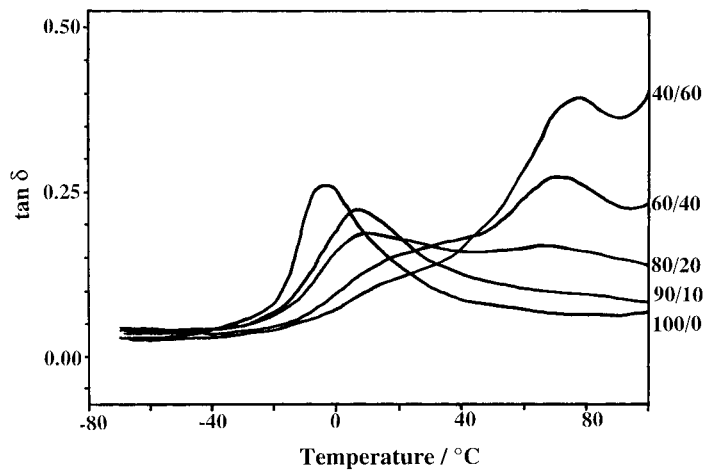


Fig. 6. Loss tangent of PB-1/HOCP blends.

Table 1

Glass-transition temperatures of PB-1/HOCP samples measured by DSC (uncertainty $\pm 2^\circ\text{C}$) and by DMTA (uncertainty $\pm 2^\circ\text{C}$)

PB-1/HOCP (w/w)	T_g ($^\circ\text{C}$) (DSC)		T_g ($^\circ\text{C}$) (DMTA)	
100/0		-23		-5
90/10	-15 ^a	— ^b	5 ^a	60–70 ^b
80/20	-10 ^a	— ^b	10 ^a	60–70 ^b
60/40	-10 ^a	— ^b	10 ^a	70 ^b
40/60	-10 ^a	— ^b	10 ^a	70 ^b
0/100		85		115 ^c

^a Glass transition of the PB-1-rich phase.

^b Glass transition of the HOCP-rich phase, not detectable by the DSC because masked by crystallization peaks (see text).

^c Extrapolated value obtained from $\tan \delta$ data of P4MP1/HOCP system [9].

the PB-1 and 90/10 blends, while the second one, not present in the specimens with a lower HOCP content, is broad and extends over the range 60–70 $^\circ\text{C}$. On increasing the HOCP content in the blend (see the 60/40 and 40/60 blends), the first peak decreased in size, whereas the second peak became larger with a well defined maximum centered at 70 $^\circ\text{C}$. The measured T_g values are reported in Table 1.

DMTA analyses are accounted for by assuming that PB-1 and HOCP were partially miscible; the two amorphous phases are one rich in PB-1 and the other one rich in HOCP. The continuous phase observable in

the optical micrographs was constituted by PB-1 and by a small amount of HOCP and its T_g is revealed by the first peak of the $\tan \delta$. The presence of HOCP in the PB-1-rich phase produced a shift of T_g to a higher temperature respect to that of the neat PB-1 because the T_g of HOCP was higher than that of PB-1 (see Table 1). The droplets observed in the melts of the blends are constituted by the HOCP-rich phase, whose glass transition was revealed by the second peak of $\tan \delta$ and increased in size as the amount of the second phase was increased, due to the addition of HOCP.

The DSC thermo-analytical curves of PB-1 and of the blends from -80 to 200 $^\circ\text{C}$ are presented in Fig. 7. As reported in the experimental part, these scans were performed on 'quenched' samples. The quenched blends contained, depending on their composition, the crystallizable PB-1 component partially or completely in the amorphous phase, which crystallized only during the DSC scanning. The PB-1 thermo-analytical curve shows the presence of a T_g at ca. -23 $^\circ\text{C}$ (see Table 1) and an endothermic peak with a maximum at ca. 120 $^\circ\text{C}$. For the blends, a single T_g value was always observed. For the 90/10 blend the T_g value is -15 $^\circ\text{C}$ and for the 80/20 to 40/60 blends the T_g values were slightly higher and independent of composition. In fact for these blends a T_g value of -10 $^\circ\text{C}$ was obtained. This transition corresponds to the first peak of the $\tan \delta$ curves, and is due to the glass transition of the PB-1-rich phase. Its value in the

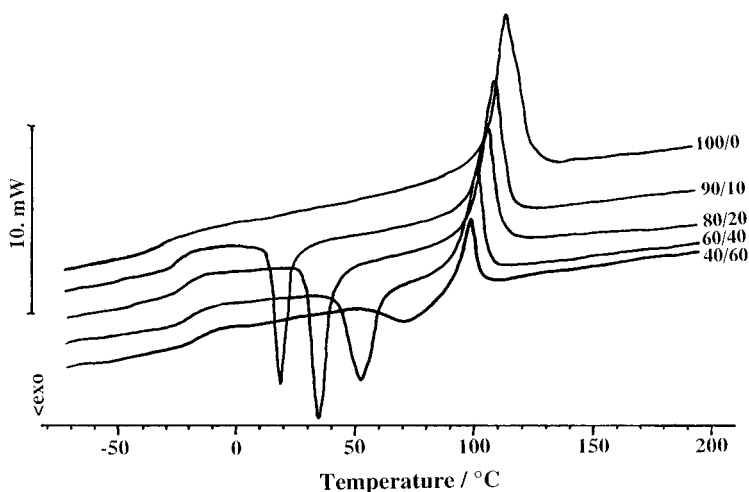


Fig. 7. DSC thermo-analytical curve of PB-1/HOCP blends performed after cooling the samples at 50 $^\circ\text{C}/\text{min}$.

blends was higher than that of neat PB-1 because of the small amount of HOCP dissolved in this phase.

For the ‘quenched’ blends, the second glass transition (due to the relaxation of the HOCP-rich phase) cannot be observed in the DSC thermoanalytical curves because it is probably masked by the presence of the exothermic peak due to crystallization of the crystallizable PB-1.

3.3. Crystallization and melting behavior

Besides the observation of the glass-transition temperature, the thermoanalytical curves presented in Fig. 7 are also remarkable for another feature. They indicate that the crystallization process of PB-1, during the quenching, was dependent on composition. In fact, when cooled at 50°C/min, the crystallizable PB-1 crystallizes completely, as shown by the presence of the single melting peak of Fig. 7. For the 90/10 blend, the crystallization was only partially avoided by quenching. In fact, in the thermoanalytical curve a crystallization peak is also present. The area under the crystallization peak is smaller than that of the melting one, indicating that not all the PB-1 crystallized during cooling. For the blends with higher HOCP content ($\geq 20\%$), both peaks had equal amplitude, indicating that the blends can be quenched to a completely

amorphous material. Moreover, it can be noted that the position of the crystallization peak changed with composition, shifting to higher temperatures with higher HOCP content. Therefore, HOCP seems to hinder the crystallization of the polyolefin.

In Fig. 8, the half time of crystallization of all samples as a function of temperature is presented. The addition of HOCP allowed PB-1 to crystallize isothermally at lower temperatures and caused a reduction in the crystallization rate. For a given crystallization temperature T_c , the increase of the time required for the crystallization can be attributed to the presence of the HOCP-rich phase in the melt. This influenced the energy related to the transport of the macromolecules to the growing crystals.

In Fig. 9, the experimentally measured melting temperatures versus the crystallization temperatures are shown. For pure PB-1, T_m increased with temperature, following the Hoffman and Weeks relationship [16]

$$T_m = \left(1 - \frac{1}{\gamma}\right)T_m^0 + \frac{T_c}{\gamma} \quad (1)$$

where T_m^0 is the equilibrium melting temperature and γ a morphological factor.

For the PB-1/HOCP system, the observed T_m values decreased with increase of HOCP, but surprisingly

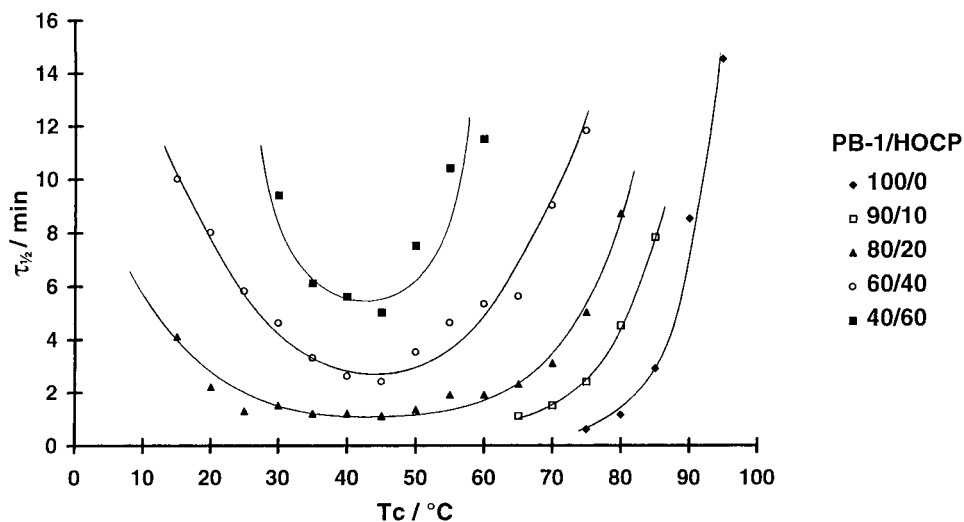


Fig. 8. Half-life of crystallization, $\tau_{1/2}$, versus crystallization temperature, T_c , for PB-1/HOCP blends.

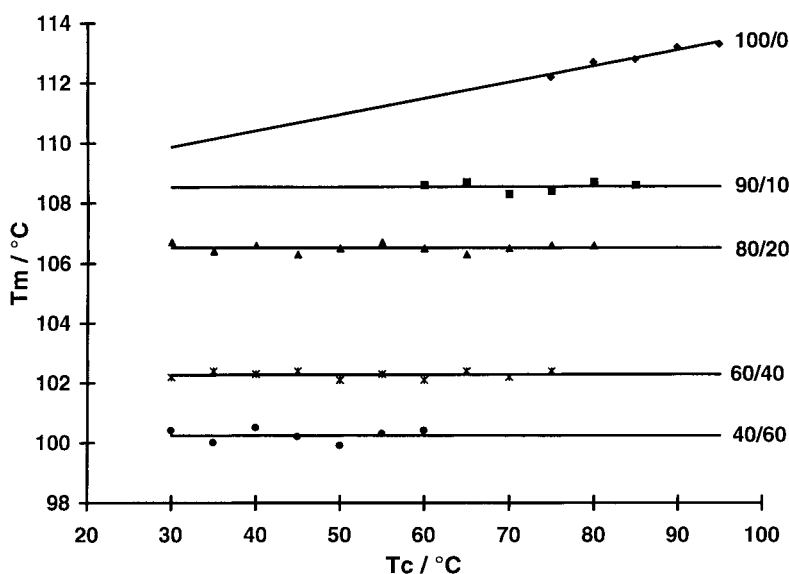


Fig. 9. Melting temperature (T_m) as a function of crystallization temperature (T_c) for PB-1/HOCP blends.

they were not affected by the crystallization temperature. Taking into account that the system crystallized from a phase-separated melt, the decrease of the observed T_m with composition is certainly due to kinetic effects. During crystallization, the presence of HOCP-rich phase disturbed the formation of PB-1 crystals. Less perfect crystals, with a lower T_m , could result and the PB-1 crystallinity decreased (see Table 2). The constancy of T_m with T_c for a given composition is more difficult to explain. Excluding the possibility of extended chain crystallization, since PB-1 has a high molecular mass, thickening of crystal lamella through annealing could be invoked. Small angle X-ray scattering work is in progress in order to

elucidate the invariance of T_m with T_c . However, Hoffman [17] recently reported that the relation (1) is valid only at low and moderate undercooling. At large undercoolings, as those used for the crystallization of the PB-1/HOCP blends, a region where T_m versus T_c is roughly constant can be predicted for a considerable range of low T_c [17].

4. Conclusions

The experimental results support the hypothesis that the miscibility grade of PB-1 and HOCP components lies between those of the polymer pairs iPP/HOCP and P4MP1/HOCP. In fact the two components were found to be partially miscible, but the two-phase region was more extended than that of the iPP/HOCP system. For the latter system, the upper and lower cloud point curves were found inside the temperature range investigated. The PB-1/HOCP system with blends of HOCP content $\geq 20\%$ always showed phase separation up to 350°C , indicating that the probable upper curve is much above this temperature. In comparison to the P4MP1/HOCP system, whose components were found to be not miscible at any composition and at any temperature investigated,

Table 2

Crystallinity index (X_c) normalized to the PB-1 content, of the isothermally crystallized samples

PB-1/HOCP (w/w)	X_c (%)
100/0	41
90/10	36
80/20	34
60/40	33
40/60	32

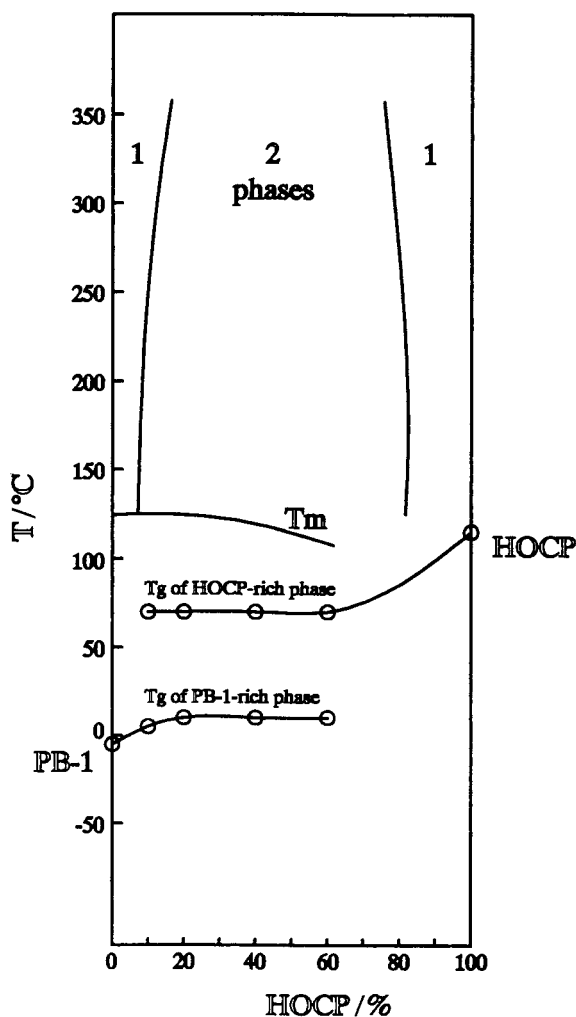


Fig. 10. Non-equilibrium phase diagram of PB-1/HOCP system.

the 90/10 PB-1/HOCP blend was miscible at $T \geq 270^\circ\text{C}$ and the blends with higher HOCP content showed the presence of two conjugated phases at all temperatures investigated, indicating partial miscibility.

The different miscibility behavior among the polymer pairs iPP/HOCP, PB-1/HOCP and P4MP1/HOCP can be ascribed to the diverse side group R of the polyolefins, since any specific interaction between the components of each polymer pair is not possible. From iPP, PB-1 to P4MP1 there is an increase of the volume units of the polyolefins and this corresponds to con-

spicuous differences in the free volume and thermal expansion coefficients. As shown by McMaster [10], the immiscible region increases with the difference in the thermal expansion coefficients of the blend components.

According to the experimental results, a pseudo-phase diagram for PB-1/HOCP system is proposed in Fig. 10. It must be noted that the data reported in Fig. 10 are not equilibrium thermodynamic values, since the values depend on the scanning rate used.

The area (labeled 1) indicates the temperature-composition range where the components are supposed to be miscible in the melt. The region 2 indicates the area where the system shows phase separation giving two conjugated phases, a PB-1-rich phase and a HOCP-rich phase. The figure also shows two T_g values (of DMTA) found for the blends whose nominal composition lies inside the two-phase region. The T_m curve describes the decrease of the melting point observed for the quenched blends with HOCP.

References

- [1] I.D. Rubin, Poly(1-Butene), H. Morawtz (Ed.), Gordon and Breach Science Publisher Ltd., London, 1968, Preface, p. vii.
- [2] P. Parrini, G. Crespi, Encyclopedia of Polymer Science and Technology, in: H.F. Mark, N.G. Gaylord, N.M. Bikales (Eds.), John Wiley and Sons, Inc., New York, 1970, vol. 13, p. 117.
- [3] S. Cimmino, E. Di Pace, E. Martuscelli, L.C. Mendes, C. Silvestre, Polym. J. Sci.: Part B: Polym. Phys. 32 (1994) 2025.
- [4] S. Cimmino, E. Di Pace, E. Martuscelli, C. Silvestre, L.C. Mendes, G. Bonfanti, J. Polym. Sci.: Part B: Polym. Phys. 33 (1995) 1723.
- [5] E. Martuscelli, C. Silvestre, M. Canetti, C. de Lalla, A. Bonfatti, A. Seves, Makromol. Chem. 190 (1989) 2615.
- [6] S. Cimmino, P. Guarrata, E. Martuscelli, C. Silvestre, Polymer 32 (1991) 3299.
- [7] S. Cimmino, E. Di Pace, F.E. Karasz, E. Martuscelli, C. Silvestre, Polymer 34 (1993) 972.
- [8] S. Cimmino, E. Martuscelli, C. Silvestre, Makromol. Chem. Macromolecular Symposia 78 (1994) 115.
- [9] S. Cimmino, M. Monaco, C. Silvestre, J. Polym. Sci.: Part B: Polym. Phys. 35 (1997) 1269.
- [10] L.P. McMaster, Macromolecules 6 (1973) 760.
- [11] P. Buzio, S. Cimmino, E. Martuscelli, P. Guarrata, C. Silvestre, Italian Patent 21834, November 1990 (to CNR Italy).

- [12] P. Buzio, B. Marcandalli, E. Martuscelli, A. Seves, Italian Patent 22196A, November 1990 (CNR Italy).
- [13] P.H. Geil, *Polymer Single Crystals*, Interscience, New York, 1961.
- [14] R.C. Allen, L. Mandelkern, *J. Polym. Sci.: Polym. Phys.* 20 (1982) 1465.
- [15] G. Bodor, *Structural Investigation of Polymers*, Ellis Horwood Limited, New York, 1991, p. 174.
- [16] J.D. Hoffman, J.J. Weeks, *J. Res. Natl. Bur. Stand., Sect. A* 66 (1962) 13.
- [17] J.D. Hoffman, R.L. Miller, *Polymer* 38 (1997) 3151.